

Linearized phase-modulated analog photonic link with the dispersion-induced power fading effect suppressed based on optical carrier band processing

DAN ZHU, JIAN CHEN, AND SHILONG PAN*

The Key Laboratory of Radar Imaging and Microwave Photonics, Ministry of Education, Nanjing University of Aeronautics and Astronautics, Nanjing 210016, China

*pans@ieee.org

Abstract: A linear phase-modulated photonic link with the dispersion-induced power fading effect suppressed based on optical carrier band (OCB) processing is proposed. By introducing a proper phase shift to the OCB, the third-order intermodulation distortion (IMD3) component of the signal transmitted over a length of fiber is effectively suppressed, while the fundamental component is shifted to be away from the notch point of the transmission response. The IMD3 and the dispersion-induced power fading effect are effectively suppressed simultaneously to realize a linear phase-modulated photonic link, and the simplicity is preserved. Theoretical analyses are taken and an experiment is carried out. Simultaneous suppression of IMD3 and dispersion-induced power fading effect is achieved. An improvement of larger than 10 dB in third-order spurious-free dynamic range (SFDR3) for both the RF frequency around the notch point and the peak point of the transmission response curve for a 20-km link is realized, as compared with the traditional phase-modulated photonic link without the OCB processing.

© 2017 Optical Society of America

OCIS codes: (060.5625) Radio frequency photonics; (060.2360) Fiber optics links and subsystems; (070.1170) Analog optical signal processing.

References and links

1. J. Capmany and D. Novak, "Microwave photonics combines two worlds," *Nat. Photonics* **1**(6), 319–330 (2007).
2. J. Yao, "Microwave photonics," *J. Lightwave Technol.* **27**(3), 314–335 (2009).
3. D. Zhu, J. Chen, and S. Pan, "Multi-octave linearized analog photonic link based on a polarization-multiplexing dual-parallel Mach-Zehnder modulator," *Opt. Express* **24**(10), 11009–11016 (2016).
4. T. R. Clark and M. L. Dennis, "Coherent optical phase-modulation link," *IEEE Photonics Technol. Lett.* **19**(16), 1206–1208 (2007).
5. Y. Shen, B. Hraimel, X. Zhang, G. E. Cowan, K. Wu, and T. Liu, "A novel analog broadband RF predistortion circuit to linearize electro-absorption modulators in multiband OFDM radio-over-fiber systems," *IEEE Trans. Microw. Theory Tech.* **58**(11), 3327–3335 (2010).
6. A. Ferreira, T. Silveira, D. Fonseca, R. Ribeiro, and P. Monteiro, "Highly linear integrated optical transmitter for subcarrier multiplexed systems," *IEEE Photonics Technol. Lett.* **21**(7), 438–440 (2009).
7. S. Li, X. Zheng, H. Zhang, and B. Zhou, "Highly linear radio-over-fiber system incorporating a single-drive dual-parallel Mach-Zehnder modulator," *IEEE Photonics Technol. Lett.* **22**(24), 1775–1777 (2010).
8. M. Huang, J. Fu, and S. Pan, "Linearized analog photonic links based on a dual-parallel polarization modulator," *Opt. Lett.* **37**(11), 1823–1825 (2012).
9. W. Li and J. Yao, "Dynamic range improvement of a microwave photonic link based on bi-directional use of a polarization modulator in a Sagnac loop," *Opt. Express* **21**(13), 15692–15697 (2013).
10. G. Zhang, S. Li, X. Zheng, H. Zhang, B. Zhou, and P. Xiang, "Dynamic range improvement strategy for Mach-Zehnder modulators in microwave/millimeter-wave ROF links," *Opt. Express* **20**(15), 17214–17219 (2012).
11. Y. Cui, Y. Dai, F. Yin, J. Dai, K. Xu, J. Li, and J. Lin, "Intermodulation distortion suppression for intensity-modulated analog fiber-optic link incorporating optical carrier band processing," *Opt. Express* **21**(20), 23433–23440 (2013).
12. P. Li, L. Yan, T. Zhou, W. Li, Z. Chen, W. Pan, and B. Luo, "Improvement of linearity in phase-modulated analog photonic link," *Opt. Lett.* **38**(14), 2391–2393 (2013).
13. J. Li, Y. C. Zhang, S. Yu, and W. Gu, "Optical Sideband Processing Approach for Highly Linear Phase-Modulation/Direct-Detection Microwave Photonics Link," *IEEE Photonics J.* **6**(5), 1–10 (2014).

14. H. Chi, X. Zou, and J. Yao, "Analytical models for phase-modulation-based microwave photonic systems with phase modulation to intensity modulation conversion using a dispersive device," *J. Lightwave Technol.* **27**(5), 511–521 (2009).
15. J. Chen, D. Zhu, and S. L. Pan, "Linearized phase-modulated analog photonic link based on optical carrier band processing", in *WOCC 2016* (2016).
16. C. H. Cox, *Analog optical links: theory and practice* (Cambridge University Press, 2006), Chap. 6.
17. M. Chen, H. Yu, and J. Wang, "Silicon Photonics-Based Signal Processing for Microwave Photonic Frontend," *Silicon Photonics III* (Springer, 2016), Chap. 11.

1. Introduction

Analog photonic links (APLs) have attracted wide attentions due to its possibility in both commercial and military applications with the advantages of low loss, wide working bandwidth, light weight and immunity to electromagnetic interference [1,2]. The spur-free dynamic range (SFDR) is a significant performance indicator for an analog photonic link. The SFDR is usually restricted by nonlinear distortions, among which the third-order intermodulation distortion (IMD3) is the primary limit of the sub-octave analog photonic link, since it is close to the RF carrier and cannot be simply removed by filters [3]. Many methods have been proposed to realize IMD3 suppression. Typical electrical methods include electrical predistortion or post processing [4,5], which is still limited by the electrical bottleneck. Photonic methods have been proposed to produce one complementary IMD3 to cancel the existing one by using a dual Mach-Zehnder modulator [6], a dual-parallel Mach-Zehnder modulator [7], or a polarization modulator [8,9], which introduce additional complexity. Recently photonic approaches using direct optical processing have been proposed to realize the IMD3 suppression [10,11]. Furthermore, direct optical processing methods have also been proposed to realize linearized phase-modulated photonic link [12,13], since the phase-modulated analog photonic link is free of bias drifting problem and has the advantages of the linear phase modulation process compared with the intensity-modulated photonic link [14]. However, extra optical bandpass filters are used in [12], which makes the system complicated and restricts the working range. In [13], appropriate phase shifts need to be imposed to both the optical carrier band (OCB) and the second-order sidebands to suppress IMD3. On the other hand, for the long-distance transmission applications, dispersion-induced power fading effect need to be solved. Few works have been done considering both the linearity and the dispersion-induced power fading effect in a photonic analog link. Recently, we have proposed a linear phase-modulated photonic link based on OCB processing, which solves the dispersion-induced power fading problem simultaneously [15]. Considering the dispersion of the transmitting fibers, the IMD3 of the signal transmitted over a length of the photonic link is power faded while maintaining the fundamental components by processing the OCB. However, only some preliminary numerical simulation results were reported in [15], which is insufficient to understand the approach.

In this paper, we perform a comprehensive theoretical and experimental study on the linear phase-modulated photonic link with the dispersion-induced power fading effect suppressed based on OCB processing. Theoretical analyses are taken and a proof of concept experiment is carried out. Simultaneous suppression of IMD3 and dispersion-induced power fading effect is achieved. The values of third-order spurious-free dynamic range (SFDR3) are larger than $102 \text{ dB}\cdot\text{Hz}^{2/3}$ for the RF frequencies around both the notch point and the peak point of the transmission response curve for a 20-km link, indicating a more than 10-dB improvement in SFDR3 as compared with the traditional phase-modulated photonic link without the OCB processing.

2. Principle

Figure 1 shows the proposed linearized phased-modulated analog photonic link with the dispersion-induced power fading effect suppressed based on OCB processing, which consists of a laser diode (LD), a phased modulator (PM), an optical carrier band (OCB) processor, a

length of single mode fiber (SMF) and a photodetector (PD). In order to characterize distortions of the analog photonic link, a common RF practice of two-tone signal analysis is taken [16]. The optical carrier with frequency of ω_0 is introduced to the PM and modulated by a two-tone RF signal with the frequencies of ω_1 and ω_2 . The two-tone signal is given by $V_m(t) = V [\cos(\omega_1 t) + \cos(\omega_2 t)]$, where V is the amplitude of the two-tone signal. The modulated optical signal at the output of the PM is as follows

$$E_{PM}(t) = E_0 \cos[\omega_0 t + m(\cos \omega_1 t + \cos \omega_2 t)] \quad (1)$$

where E_0 is the amplitude of the optical signal, $m = \pi V / V_\pi$, V_π is the half-wave voltage of the PM. It can be further expanded in terms of Bessel functions of the first kind as

$$E_{PM}(t) = E_0 \sum_{l=-\infty}^{\infty} \sum_{n=-\infty}^{\infty} \{J_l(m) J_n(m) \cos[\omega_0 t + l\omega_1 t + n\omega_2 t + 0.5\pi(l+n)]\} \quad (2)$$

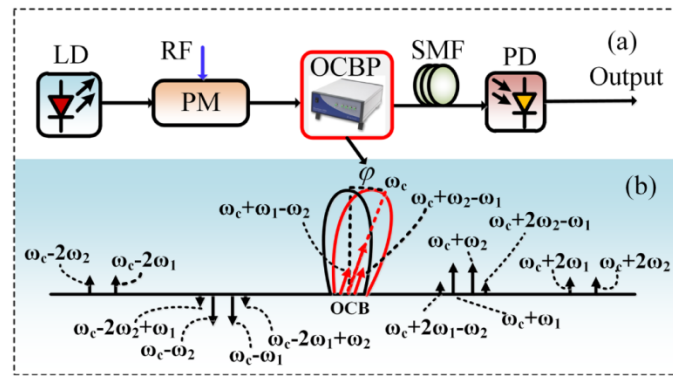


Fig. 1. (a) Schematic diagram and (b) operation principle of the proposed phase-modulated analog photonic link based on optical carrier band processing. LD: laser diode, PM: phase modulator, OCBP: optical carrier band processor, SMF: single mode fiber, PD: photodetector, OCB: optical carrier band.

As shown in Fig. 1 (b), with the OCBP introducing a phase shift of φ to the optical carrier band, the optical field of the optical carrier band can be expressed as

$$E_{OCB}(t) = E_0 \left\{ J_0^2 \cos(\omega_c t + \varphi) + J_1 J_{-1} \left[\cos((\omega_c + \omega_1 - \omega_2)t + \varphi) + \cos((\omega_c + \omega_2 - \omega_1)t + \varphi) \right] \right\} \quad (3)$$

where $J_n = J_n(m)$ ($n = 0, \pm 1$). After transmitting over a SMF with a length of L , the fiber dispersion introduces phase shift of $\theta_\omega = \beta L$, where β represents the propagation constant related to optical carrier frequency. Thus the optical field can be expressed as

$$\begin{aligned} E_{PM}(t) = E_0 \left\{ J_0^2 \cos(\omega_c t + \varphi) + J_1 J_{-1} \cos \left[(\omega_c + \omega_{1,2} - \omega_{2,1})t + \theta_{\omega_c + \omega_{1,2} - \omega_{2,1}} + \varphi \right] \right. \\ - J_1 J_0 \sin \left[(\omega_c + \omega_{1,2})t + \theta_{\omega_c + \omega_{1,2}} \right] - J_2 J_{-1} \sin \left[(\omega_c + 2\omega_{1,2} - \omega_{2,1})t + \theta_{\omega_c + 2\omega_{1,2} - \omega_{2,1}} \right] \\ + J_{-1} J_0 \sin \left[(\omega_c - \omega_{1,2})t + \theta_{\omega_c - \omega_{1,2}} \right] + J_{-2} J_1 \sin \left[(\omega_c - 2\omega_{1,2} + \omega_{2,1})t + \theta_{\omega_c - 2\omega_{1,2} + \omega_{2,1}} \right] \\ \left. - J_2 J_0 \cos \left[(\omega_c + 2\omega_{1,2})t + \theta_{\omega_c + 2\omega_{1,2}} \right] - J_{-2} J_0 \cos \left[(\omega_c - 2\omega_{1,2})t + \theta_{\omega_c - 2\omega_{1,2}} \right] \right\} \quad (4) \end{aligned}$$

where $J_n = J_n(m)$ ($n = 0, \pm 1, \pm 2$), and higher order components are ignored. By injecting the optical signal into the PD, the output electrical signal is

$$\begin{aligned}
I \propto & \cos[\omega_{1,2}(t + L\beta'(\omega_c))] \cdot J_1 J_0^3 \sin[0.5L\beta''(\omega_c)\omega_{1,2}^2 - \varphi] \\
& + \cos[(2\omega_{1,2} - \omega_{2,1})(t + L\beta'(\omega_c))] \cdot \left\{ J_1^3 J_0 \sin[\varphi + 0.5L\beta''(\omega_c)((\omega_1 - \omega_2)^2 - \omega_{1,2}^2)] \right. \\
& \quad + J_0^2 J_2 J_1 \sin[\varphi - 0.5L\beta''(\omega_c)(2\omega_{1,2} - \omega_{2,1})^2] \\
& \quad \left. + J_0^2 J_2 J_1 \sin[2L\beta''(\omega_c)\omega_{1,2}^2 - 0.5L\beta''(\omega_c)\omega_{2,1}^2] \right\} \quad (5)
\end{aligned}$$

where β' and β'' represents the 1st and 2nd derivation of β , respectively. Thus the coefficients of the fundamental and the IMD3 components are as follows

$$\begin{cases}
I_c = J_1 J_0^3 \sin[0.5L\beta''(\omega_c)\omega_{1,2}^2 - \varphi] \\
I_{IMD3} = \left\{ J_1^3 J_0 \sin[\varphi + 0.5L\beta''(\omega_c)((\omega_1 - \omega_2)^2 - \omega_{1,2}^2)] \right. \\
\quad + J_0^2 J_2 J_1 \sin[\varphi - 0.5L\beta''(\omega_c)(2\omega_{1,2} - \omega_{2,1})^2] \\
\quad \left. + J_0^2 J_2 J_1 \sin[2L\beta''(\omega_c)\omega_{1,2}^2 - 0.5L\beta''(\omega_c)\omega_{2,1}^2] \right\} \quad (6)
\end{cases}$$

Assuming $|\omega_1 - \omega_2| \ll \omega_{1,2}$, (6) can be derived as

$$\begin{cases}
I_c = J_1 J_0^3 \sin[0.5L\beta''(\omega_c)\omega_{1,2}^2 - \varphi] \\
I_{IMD3} = \left\{ (J_1^3 J_0 + J_0^2 J_2 J_1) \sin[\varphi - 0.5L\beta''(\omega_c)\omega_{1,2}^2] \right. \\
\quad \left. + J_0^2 J_2 J_1 \sin[1.5L\beta''(\omega_c)\omega_{1,2}^2] \right\} \quad (7)
\end{cases}$$

It can be seen that by setting the value of φ to be a proper value, $I_{IMD3} = 0$ while optimizing the value of I_c can be realized. In this way, the IMD3 is efficiently suppressed while the dispersion-induced power fading effect is solved simultaneously. Thus a linear phase-modulated analog photonic link with the dispersion-induced power fading effect suppressed is realized based on OCB processing.

3. Experimental results and discussions

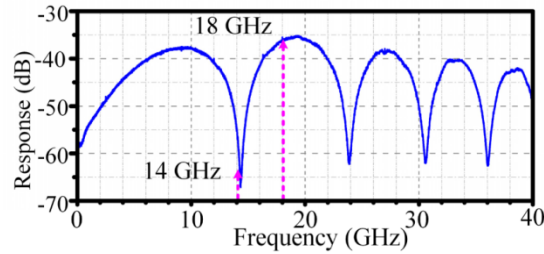


Fig. 2. The experimental transmission response of the PM based analog photonic link without introducing any phase shift to the optical carrier band.

An experiment based on the setup shown in Fig. 1 is carried out. The wavelength of the laser source (Teraxion, PS-NLL-1550.12-8004) is set to be 1550.12 nm. The phase modulator (PM, Eospace PM-DV5-40-PFU-PFU-LV) has a half voltage of 4.0 V and a 3-dB bandwidth of 30 GHz. The two-tone RF signals are generated by a microwave signal generator (Agilent E8267D). The OCBP is realized by using a commercial waveshaper (Finisar 4000s). The SMF for transmission has a length of 20 km. The PD (u²t, XPDV2120R) has a bandwidth of 50 GHz and a responsivity of 0.65 A/W. A vector network analyzer (VNA, R&S ZVA67,10

MHz-67 GHz) is used to measure the responses of the link. The electrical spectra are measured by an electrical signal analyzer (R&S FSV-40, 10 Hz ~40 GHz).

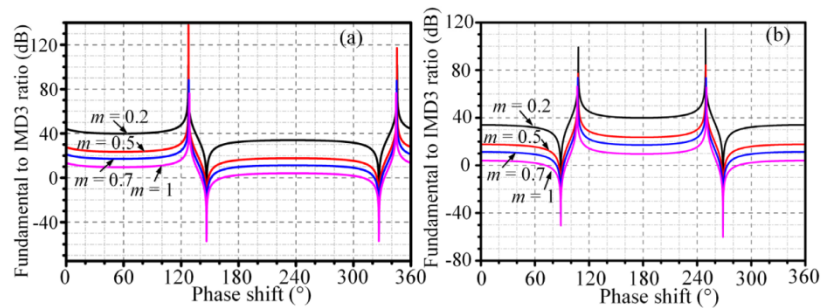


Fig. 3. The simulated fundamental to IMD3 ratio values versus the phase shift ϕ introducing to the optical carrier band for different modulation indices with the RF working frequency around (a) 18 GHz and (b) 14 GHz.

In order to demonstrate the capability of simultaneous suppression of IMD3 and dispersion-induced power fading effect, two typical different working frequencies at 14 GHz and 18 GHz are chosen in our experiment. The transmission response of the PM based analog photonic link without introducing any phase shift to the OCB is shown in Fig. 2. As can be seen, the frequency of 14 GHz and 18 GHz are around the notch point and the peak point, respectively. In order to obtain the proper values of the phase shift ϕ to realize the PM based photonic link linearization, a simulation is taken to analyze the relationship between the fundamental to IMD3 ratio and the phase shift ϕ based on Eq. (7). The second order derivation of the propagation constant is set to be $20 \text{ ps}^2/\text{km}$. As shown in Fig. 3, for different modulation indices m , a proper phase shift value exists to optimize the fundamental to IMD3 ratio, and furthermore, the proper phase shift values are almost the same for a wide modulation indices range. For the condition with RF working frequency at 18 GHz, the optimized phase shift values are shown to be around 130° or 345° , while for the condition with 14 GHz, the proper phase shift values are shown to be around 110° or 250° .

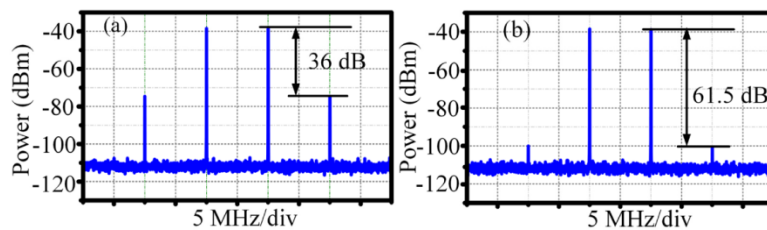


Fig. 4. Experimental electrical spectra of the output fundamental signal and their IMD3 for the 14-GHz working condition (a) without (b) with introducing a phase shift of 155° to the optical carrier band.

A two-tone signal test is taken to obtain the link performances. By introducing a two-tone RF signal with frequencies of 14.095 and 14.105 GHz to the PM, IMD3 components at frequencies of 14.085 GHz and 14.115 GHz are presented. Figure 4 shows the measured electrical spectra of the output fundamental signal and their IMD3 for the 14-GHz working condition when the RF power is set to be 6 dBm. Without introducing any phase shift to the OCB, the fundamental to IMD3 ratio is 36 dB, as shown in Fig. 4 (b). By introducing a phase shift of 155° to the optical carrier band, the fundamental to IMD3 ratio is dramatically increased to 61.5 dB, showing a 25.5-dB improvement. The SFDR performances for the two conditions are also measured by varying the modulated RF signal power, as shown in Fig. 5. The noise floor is set to be -160 dBm/Hz . As can be seen, without introducing any phase shift

to the OCB, the SFDR3 is $92.08 \text{ dB}\cdot\text{Hz}^{2/3}$. By using the proposed method and introducing a phase shift of 155° , the SFDR3 is $103.04 \text{ dB}\cdot\text{Hz}^{2/3}$. An improvement of 10.96 dB in SFDR3 is achieved. The transmission response is also measured as shown in Fig. 6. As can be seen, compared with the results in Fig. 2, the working band around 14 GHz has been shifted away from the notch point, which means that the dispersion-induced power fading effect is suppressed. Thus, the simultaneous suppression of IMD3 and the dispersion-induced power fading effect is successfully realized.

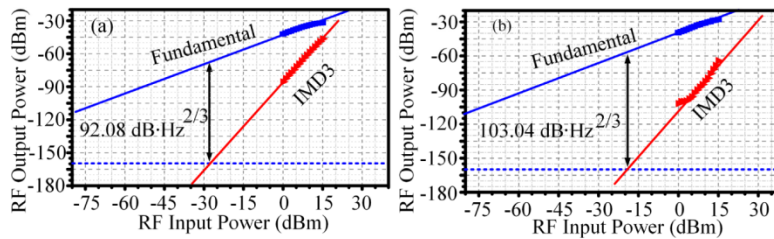


Fig. 5. Experimental SFDR performance of the PM based analog photonic link (a) without (b) with introducing a phase shift of 155° to the optical carrier band for the 14-GHz working condition.

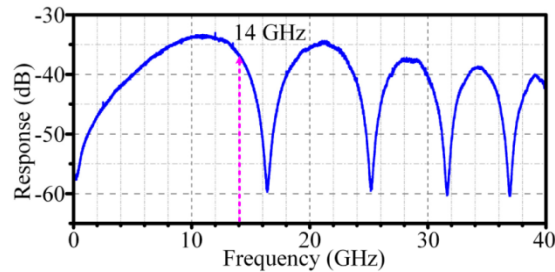


Fig. 6. The experimental transmission response of the PM based analog photonic link with introducing a phase shift of 155° to the optical carrier band.

By tuning the working frequency band to be around 18 GHz, the measured electrical spectra of the output fundamental signal and their IMD3 are shown in Fig. 7. With a two-tone RF signal with frequencies of 17.995 GHz and 18.005 GHz modulated, IMD3 components at 17.985 GHz and 18.015 GHz are presented. It can be seen that the fundamental to IMD3 ratio has an improvement of 29.41 dB by introducing a phase shift of 135° to the OCB. The measured SFDR performances are shown in Fig. 8. The SFDR3 with and without introducing a phase shift of 155° to the OCB has a value of $91.1 \text{ dB}\cdot\text{Hz}^{2/3}$ and $102.25 \text{ dB}\cdot\text{Hz}^{2/3}$, respectively, showing a 11.15-dB improvement. Thus the IMD3 is effectively suppressed and a linear phase-modulated photonic link is realized. Figure 9 shows the transmission response. Compared with the results shown in Fig. 2, it can be seen that the working band around 18 GHz is kept to be around the peak point. In our experiments, the proper phase shift value for the 18-GHz working condition agrees well with the theoretically simulated result, while the experimental phase shift value for the 14-GHz working condition has deviation with the corresponding simulated value. This is due to the processing deviation of the optical processor in actual experiments.

By using the proposed method, a linear phase-modulated analog photonic link with simultaneous suppression of dispersion-induced power fading effect is realized based on OCB processing. According to Eq. (7), it can be seen that the proper value of φ applied to the OCB is dependent on the transmission length L of the link. Thus the optical carrier band processing should be done according to the transmission length of the link. On the other hand, the system performance can be further improved if the optical processor can realize a higher processing

precision. By using an integrated optical processor [17], the simplicity and the performance of the proposed analog photonic link will be further improved.

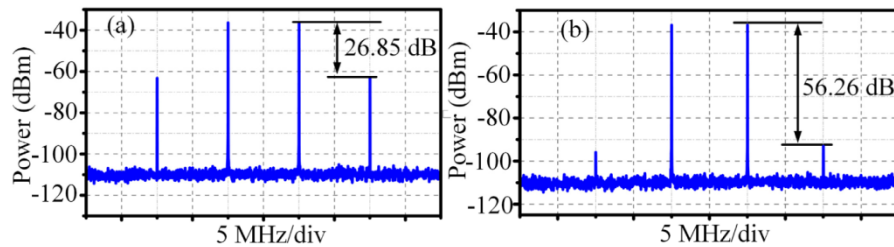


Fig. 7. Experimental electrical spectra of the output fundamental signal and their IMD3 for the 18-GHz working condition (a) without (b) with introducing a phase shift of 135° to the optical carrier band.

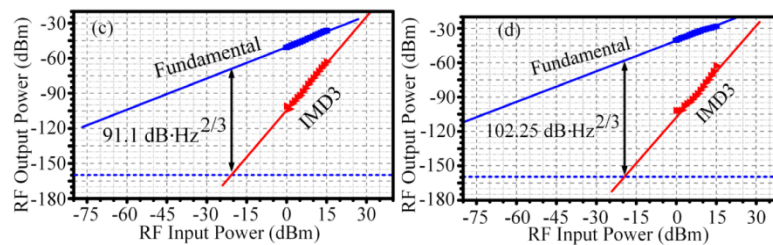


Fig. 8. Experimental SFDR performance of the PM based analog photonic link (a) without (b) with introducing a phase shift of 135° to the optical carrier band for the 18-GHz working condition.

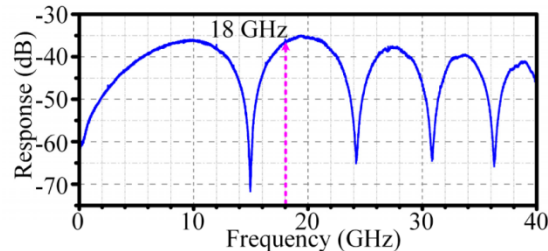


Fig. 9. The experimental transmission response of the PM based analog photonic link with introducing a phase shift of 135° to the optical carrier band.

4. Conclusion

A linear phase-modulated photonic link with the dispersion-induced power fading effect suppressed based on optical carrier band processing is proposed and demonstrated. By simply introducing a phase shift to the OCB, the IMD3 and the dispersion-induced power fading effect are effectively suppressed simultaneously. Analytical model is established, and simultaneous suppression of IMD3 and the dispersion-induced power fading effect is experimentally demonstrated. The performance is improved by larger than 10 dB in SFDR3 as compared with the traditional phase-modulated photonic link without processing of the OCB. This approach can be applied for long-distance transmission with linearity in both commercial and military systems.

Funding

National Natural Science Foundation of China (NSFC) (61422108); Natural Science Foundation of Jiangsu Province (BK20160082); Jiangsu Provincial Program for High-level Talents in Six Areas (DZXX-030).